



## White matter microstructure associations to amyloid burden in adults with Down syndrome

Austin M. Bazydlo<sup>a,\*</sup>, Matthew D. Zammit<sup>a</sup>, Minjie Wu<sup>c</sup>, Patrick J. Lao<sup>a</sup>, Douglas C. Dean III<sup>a,b</sup>, Sterling C. Johnson<sup>a</sup>, Dana L. Tudorascu<sup>c</sup>, Ann Cohen<sup>c</sup>, Karly A. Cody<sup>a</sup>, Beau Ances<sup>d</sup>, Charles M. Laymon<sup>c</sup>, William E. Klunk<sup>c</sup>, Shahid Zaman<sup>e</sup>, Benjamin L. Handen<sup>c</sup>, Sigan L. Hartley<sup>b</sup>, Andrew L. Alexander<sup>a,b</sup>, Bradley T. Christian<sup>a,b</sup>

<sup>a</sup> School of Medicine and Public Health, University of Wisconsin-Madison, Madison, WI, USA

<sup>b</sup> Waisman Center, Wisconsin Alzheimer's Disease Research Center, University of Wisconsin-Madison, Madison, WI, USA

<sup>c</sup> University of Pittsburgh School of Medicine, Pittsburgh, PA, USA

<sup>d</sup> Washington University, St. Louis, MO, USA

<sup>e</sup> Cambridge Intellectual and Developmental Disabilities Research Group, University of Cambridge, Cambridge, United Kingdom

### ARTICLE INFO

#### Keywords:

Down syndrome  
Alzheimer's Disease  
DTI  
PET  
Amyloid- $\beta$

### ABSTRACT

**Introduction:** Individuals with Down syndrome (DS) are at an increased risk of developing Alzheimer's Disease (AD). One of the early underlying mechanisms in AD pathology is the accumulation of amyloid protein plaques, which are deposited in extracellular gray matter and signify the first stage in the cascade of neurodegenerative events. AD-related neurodegeneration is also evidenced as microstructural changes in white matter. In this work, we explored the correlation of white matter microstructure with amyloid load to assess amyloid-related neurodegeneration in a cohort of adults with DS.

**Methods:** In this study of 96 adults with DS, the relation of white matter microstructure using diffusion tensor imaging (DTI) and amyloid plaque burden using [<sup>11</sup>C]PiB PET were examined. The amyloid load (A $\beta$ <sub>T</sub>) derived from [<sup>11</sup>C]PiB was used as a global measure of amyloid burden. A $\beta$ <sub>T</sub> and DTI measures were compared using tract-based spatial statistics (TBSS) and corrected for imaging site and chronological age.

**Results:** TBSS of the DTI maps showed widespread age-by-amyloid interaction with both fractional anisotropy (FA) and mean diffusivity (MD). Further, diffuse negative association of FA and positive association of MD with amyloid were observed.

**Discussion:** These findings are consistent with the white matter microstructural changes associated with AD disease progression in late onset AD in non-DS populations.

### 1. Background

Down syndrome (DS) is a genetic disorder involving trisomy of chromosome 21 resulting in an overproduction of various proteins encoded from this chromosome, including amyloid precursor protein (APP) (Wiseman et al., 2015). As one of the neuropathological features of Alzheimer's disease (AD), an overproduction of APP and accompanying amyloid-beta (A $\beta$ ) pathology are implicated as primary sources for the enhanced risk of AD in individuals with DS (Wiseman et al., 2015). As the life expectancy of people with DS nearly quadrupled in the last century, from 16 years of age in the early 20th century to 60 years in 2019 (Zigman et al., 2008) the prevalence of AD in this population has

increased in parallel, with a lifetime risk of approximately 90% (McCarron et al., 2014).

Positron emission tomography (PET) imaging studies have been used to characterize amyloid burden in DS populations and have shown increased retention of [<sup>11</sup>C]PiB (Pittsburgh compound B), which preferentially binds to amyloid plaques, in some participants by their fourth decade (30–40 years) of life and the majority with amyloid positivity (amyloid(+)) by the middle of their fifth decade (Annus et al., 2016; Lao et al., 2016). These findings reveal the emergence of PET-measured amyloid(+) status in DS approximately 30 years earlier than seen in the general (non-DS) population. However, similar to the general population, the early stages of amyloid accumulation in DS do not adversely

\* Corresponding author at: University of Wisconsin-Madison, Department of Medical Physics, 1500 Highland Ave, Madison, WI 53705, USA.

E-mail address: [ambazydlo@gmail.com](mailto:ambazydlo@gmail.com) (A.M. Bazydlo).

<https://doi.org/10.1016/j.nicl.2021.102908>

Received 10 February 2021; Received in revised form 25 October 2021; Accepted 3 December 2021

Available online 10 December 2021

2213-1582/© 2021 Published by Elsevier Inc. This is an open access article under the CC BY-NC-ND license (<http://creativecommons.org/licenses/by-nc-nd/4.0/>).

affect cognitive function. In a study of non-demented DS participants (age 30–53), there were no significant differences in neuropsychological measures across amyloid(+) and amyloid(–) groups (Hartley et al., 2014).

There are relatively few structural magnetic resonance imaging (MRI) studies of aging-DS and these studies have revealed varying results (Neale et al., 2018). Detectable changes of gray matter volume and glucose metabolism with increased amyloid were observed by Matthews et al. (2016) and Raffi et al. (2015) in non-demented individuals with DS. Recently, Lao et al. (2018) studied a group of non-demented individuals with DS using structural MRI and PET and found no indication of pre-AD changes in MRI-measured gray matter morphology between amyloid(+) and amyloid(–) participants. Similar to the temporal course of AD biomarkers in the general population, these studies confirm that amyloid accumulation precedes gray matter atrophy and clinical dementia onset in DS (Zammit et al., 2020b). This order of events is consistent with the AT(N) model (amyloid → tau → neurodegeneration) describing the progression of AD-related biomarkers (Jack et al., 2018). Neurodegeneration is typically characterized by MRI-measured atrophy in the hippocampus or FDG PET patterns of hypometabolism in the precuneus, temporal and parietal cortices. Research is also ongoing to employ other neuroimaging modalities such as diffusion tensor imaging (DTI) to characterize microstructural changes in subcortical white matter related to neurodegeneration.

Diffusion tensor imaging (DTI) is a non-invasive MRI technique used to probe microstructural differences in water diffusion properties of biological tissues (Basser et al., 1994; Basser and Pierpaoli, 1996). DTI measurements include the mean diffusivity (MD), which is the directionally averaged diffusivity and is sensitive to the density of microstructural features; and the fractional anisotropy (FA), which is a summary measure of the directional variance of diffusivities and is often used as a sensitive marker of white matter microstructural changes (Alexander et al., 2007). Although AD is often considered a disease of gray matter, white matter degeneration is also observed. This finding has been confirmed in several studies (Mayo et al., 2017; Nowrangi et al., 2013; Nowrangi et al., 2015; O'Dwyer et al., 2011) that have used DTI to compare AD subjects to healthy controls. DTI investigations of white matter integrity in AD populations have reported increased MD and decreased FA in multiple white matter regions across the brain (Mayo et al., 2018; Mayo et al., 2017; Nowrangi et al., 2015). These outcomes have been associated with cognitive decline and impaired executive function resulting from the deterioration of cortico-limbic, entorhinal, and cortico-cortico connections, potentially resulting from the presence of A $\beta$  and NFTs.

Previous DTI studies of non-demented individuals with DS have reported reduced FA relative to typically developing controls in frontal white matter connections (Fenoll et al., 2017; Romano et al., 2018). Similarly, Powell et al. (2014) observed widespread FA decreases in the frontal lobe in demented individuals with DS compared with non-demented individuals with DS and age-matched controls.

Several neuroimaging studies have also investigated the relationships between early white matter microstructural changes in AD and amyloid burden with PiB PET (Chao et al., 2013; Racine et al., 2014; Wolf et al., 2015). The goal of this study was to examine these relationships within an aging DS population, which is an important first step to evaluate whether DTI may be a sensitive marker to the microstructural changes in the early stages of A $\beta$  deposition before evidence of GM degradation and cognitive decline. Given the near certainty of AD development and wide range of disease trajectories in individuals with DS and the marked early onset of pathology, characterizing the relationships between early white matter changes and amyloid burden in DS is essential to better understand disease progression. In this work, we investigated the relationships between [ $^{11}\text{C}$ ]PiB-measured amyloid burden in the brain with DTI measurements to assess white matter microstructure changes, as well as the effects of age on these changes, in a cohort of individuals with Down syndrome.

## 2. Methods

### 2.1. Participant selection

Ninety-six ( $n = 96$ ) individuals with Down syndrome (average age  $38.45 \pm 7.98$  yrs.) received baseline scans as part of the Alzheimer's Biomarker Consortium-Down Syndrome (ABC-DS) study at three imaging facilities (34 at the University of Wisconsin-Madison, 34 at the University of Pittsburgh Medical Center (UPMC), and 28 at the University of Cambridge (UC)). All participants had genetically confirmed trisomy 21. Eleven participants were excluded due to excessive artifacts in the raw diffusion-weighted images. Artifacts were identified using automated signal outlier detection using the FSL eddy command with the –repol option (Andersson et al., 2016; Andersson and Sotiropoulos, 2016). Diffusion-weighted volumes were rejected if more than 10% of the slices demonstrated outliers. Subjects were excluded if more than 10% of the diffusion-weighted volumes were rejected. Of the remaining 85 participants, 78 were classified as non-demented (i.e., cognitively and functionally stable); 4 were classified as having mild cognitive impairment (MCI), and 3 participants were classified as demented. These clinical status determinations were based on a case consensus process that included at least three staff with clinical expertise who were blind to MRI and PET imaging data. Informed consent was obtained prior to data collection.

The following information was used in the case consensus process: a) medical/psychiatric history and neurological exam; b) caregiver-report of participant's functioning and life events; c) participant's adaptive skills on the Vineland Adaptive Behavior Scales (2012; Sparrow et al., 1984); d) caregiver-report of participant's dementia symptoms on Dementia Questionnaire for People with Learning Disabilities (Evenhuis, 2018) or Dementia Scale for Down syndrome (Jozsvai et al., 2018); e) participant's profile on the Down Syndrome Mental Status Examination (Haxby, 1989b), Developmental Test of Visual-Motor Integration, 5th Edition (Beery, 2004), Wechsler Intelligence Scale for Children (Wechsler, 1945) Block Design and Haxby extension (Haxby, 1989a), and Developmental NeuroPsychological Assessment (Korkman et al., 2007) Word Generation Semantic Fluency.

Analyses were performed both with and without the subjects classified as either MCI or demented. Removal of these subjects did not result in a loss of significant effects, so subjects were included for increased statistical power.

#### 2.1.1. PET imaging of amyloid burden

A target dose of 15 mCi of [ $^{11}\text{C}$ ]PiB was delivered intravenously while participants were resting outside the PET scanner. PET data were acquired following a 40-minute radiotracer uptake period using either a Siemens ECAT HR+ (UW and UPMC), a Siemens 4-ring Biograph mCT (UPMC), or GE Advance (UC) scanner. The time-series acquisition was performed from 40 to 70 min (post-injection) with data binned into 5-minute time frames. PET images were reconstructed with the ECAT system software (OSEM algorithm; 4 iterations, 16 subsets) to a voxel size of  $2.57 \text{ mm} \times 2.57 \text{ mm} \times 2.43 \text{ mm}$  and matrix dimension of  $128 \times 128 \times 63$  with corrections for detector deadtime, scanner normalization, photon attenuation and scatter, and radioactive decay. PET scans were reoriented along the anterior commissure posterior commissure (AC-PC) line, and inter-frame motion was corrected (Woods et al., 1998). Standard uptake value ratio (SUVR) images were calculated from PET data 50–70 min post-injection (McNamee et al., 2009) with a cerebellar gray matter reference region. (Klunk et al., 2004; Lopresti et al., 2005; Price et al., 2005) Global A $\beta$  burden was calculated using the amyloid load metric (A $\beta_L$ ) following previously described methodology (Zammit et al., 2020a).

#### 2.1.2. Diffusion tensor imaging

MRI data were collected on 3.0T MRI scanners - a GE SIGNA 750 with an 8-channel head coil (UW-Madison), a Siemens Magnetom Trio

scanner with a 64-channel head coil (UPMC), a GE Signa PET-MR scanner with a 32-channel head coil (UC). Diffusion-weighted imaging at both sites was performed using a single-shell, diffusion-weighted spin echo sequence (UW-Madison TR/TE = 7800/67 ms; UPMC TR/TE = 7200/56 ms; UC TR/TE = 15707/75 ms). The DWI protocol consisted of either 7 (UPMC) or 6 (UW-Madison and UC) non-diffusion weighted ( $b_0$ ) images and diffusion weighted images with a b-value of 1000 s/mm<sup>2</sup> in 48 non-collinear directions. Additional imaging parameters consisted of matrix size: 116 × 116, field of view: 23.2 × 23.2 × 16 cm<sup>3</sup>, and 80 2 mm thick slices. Data were processed using an in-house processing pipeline utilizing tools from FSL (Jenkinson et al., 2012), MRTrix3 (Tournier et al., 2019), and the DiPy toolbox (Garyfallidis et al., 2014). The diffusion-weighted data were corrected for Gibbs' ringing artifacts (Kellner et al., 2016), Gaussian noise (Veraart et al., 2016), and eddy

current distortions and head motion with outlier replacement (Andersson et al., 2016; Andersson and Sotiropoulos, 2016). A threshold of 10% or more of slices replaced as outliers within a single diffusion weighted image was established as a criterion for removal of a volume; however, no volumes exceeded this threshold and no DWIs were removed. The diffusion tensors were estimated using a robust estimator method, RESTORE (Chang et al., 2005), and FA and MD maps subsequently calculated.

## 2.2. Statistical analyses

### 2.2.1. Tract-based spatial statistics

Statistical analyses of the DTI data were performed using the tract-based spatial statistics (TBSS) pipeline in FSL (Smith et al., 2006;

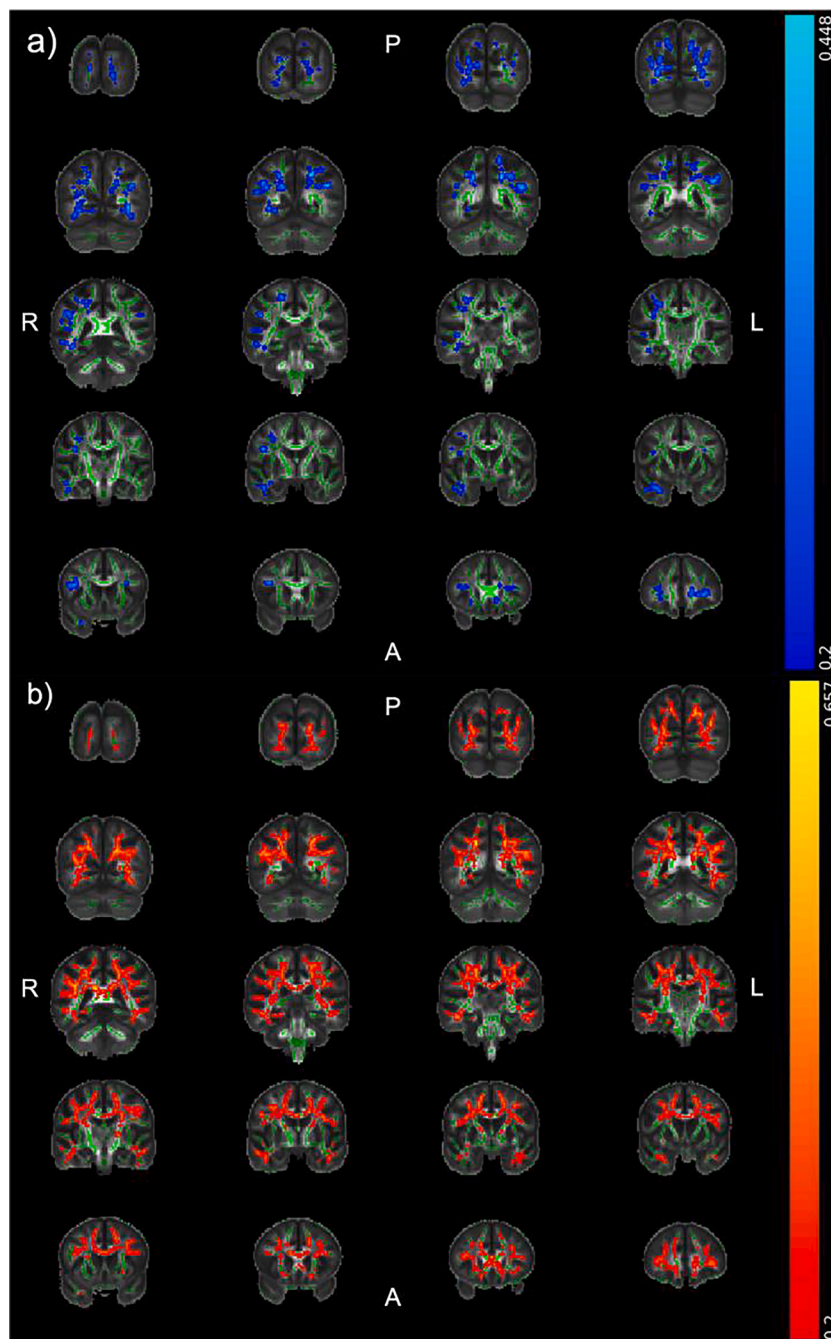


**Fig. 1.** a) areas of significant negative correlation between FA and AβL. b) Regions of significant correlation between MD and AβL. Results reflect regions with  $p < 0.05$  corrected for multiple comparisons, imaging site, and age.

Smith et al., 2004).

2.2.2. Statistical testing

A general linear model (GLM) was constructed in FSL to investigate voxel-wise correlations of FA and MD with amyloid load,  $A\beta_L$ . These analyses were completed using the FSL tool PALM with threshold-free cluster enhancement (TFCE) to identify significant brain regions. Correction for multiple comparisons was performed by controlling for the Family-Wise Error rate (Smith and Nichols, 2009). For all TBSS results, the FSL tool *tbss\_fill* was used for ease of visualization; all inflated regions were mapped from a corrected significance of  $p < 0.05$ .

A general linear model (GLM) was constructed in FSL to investigate voxel-wise comparisons of continuous  $A\beta_L$ -by-age ( $A\beta_L$ \*age) interactions of DTI measures projected onto the population derived FA. A

mask of areas with significant  $A\beta_L$ \*age interaction was generated and used to extract average MD and FA values from within these areas.

3. Results

Significantly decreased and widespread FA with increased  $A\beta_L$  is shown in Fig. 1a (blue regions), which includes the bilateral occipital and prefrontal white matter, as well as the genu of the corpus callosum, the right superior longitudinal fasciculus, the fornix, and left inferior longitudinal fasciculus. These regions in Fig. 1a were generated with a site covariate and age correction. Likewise, Fig. 1b shows regions of significant positive correlation of  $A\beta_L$  and MD. Across the extent of the significant regions shown, FA and MD were correlated with  $A\beta_L$  at  $r = -0.611$  ( $p < 0.001$  corrected) and  $r = 0.552$  ( $p < 0.001$  corrected),

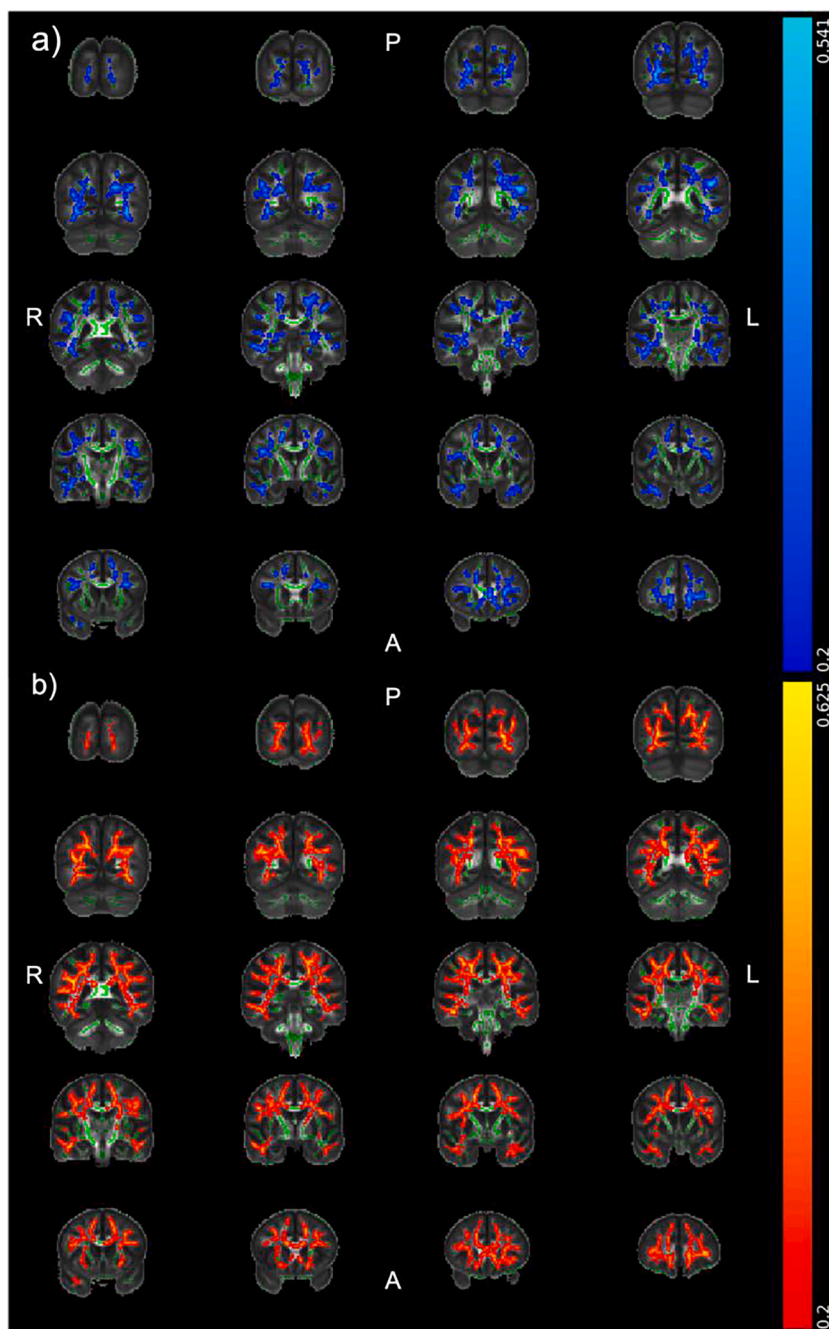


Fig. 2. a) Regions of significant negative  $A\beta_L$ \*age interaction with FA. b) Regions of significant  $A\beta_L$ \*age interaction with MD. Results reflect regions with  $p < 0.05$  corrected for multiple comparisons and imaging site.

respectively.

Fig. 2a shows a negative  $A\beta_L$ \*age interaction with FA. Fig. 2b reveals regions of positive  $A\beta_L$ \*age interaction with MD. Results are mapped at a significance of  $p < 0.05$  corrected for multiple comparisons and imaging site. Across the extent of the significant regions shown, FA and MD were correlated with  $A\beta_L$ \*age at  $r = -0.606$  ( $p < 0.001$  corrected) and  $r = 0.623$  ( $p < 0.001$  corrected), respectively. No significant positive  $A\beta_L$ \*age interactions with FA, nor were any significant negative  $A\beta_L$ \*age interactions with MD observed.

#### 4. Discussion

To our knowledge, this is the first study to investigate the white matter microstructural differences based upon amyloid burden in individuals with DS. Our findings reveal a positive relation of MD with amyloid over most of the association white matter pathways. Further, our cohort exhibited diffuse negative associations of FA with  $A\beta_L$  in the bilateral occipital parietal and prefrontal white matter, the genu of the corpus callosum, and right temporal white matter and right superior longitudinal fasciculus. Site was included as a co-variate, with significant site effects found in the cerebellum, brainstem, posterior-inferior WM tracts for FA and the corpus callosum and corona radiata for MD. Importantly, independent analyses for each site showed similar correlations of interactions of FA and MD with  $A\beta_L$ . As the effects were preserved in the individual site analyses, we conclude that a site covariate within the GLM was sufficient to mitigate scanner-specific effects and no further data harmonization was needed. Since the effects are so widespread across the white matter, particularly for MD, adding other diffusion-weighted measures was not necessary to demonstrate that widespread microstructural changes are related to aging and amyloid burden in Down syndrome, thus are not included here. Further, the single-shell diffusion-weighted imaging protocol prohibited more advanced diffusion models such as either diffusion kurtosis imaging (DKI) or neurite orientation dispersion and density imaging (NODDI).

Caballero et al. (2020) observed a significant amyloid-age interaction of MD and white matter hyper intensity volume in a cohort of non-DS, non-AD individuals, which suggested an accelerated neurodegeneration in subjects with greater amyloid and is in line with our findings in aging DS (Caballero et al., 2020). It is well documented in geriatric imaging studies that white matter FA decreases with age and MD increases (Abe et al., 2002; Bennett et al., 2010; Hsu et al., 2008). Given the trend of FA to decrease and MD to increase in prodromal and fully realized AD relative to healthy controls, our findings suggest that individuals with DS with significant amyloid show signs of neurodegeneration, similar to the findings of Caballero et al. (2020).

The association between white matter microstructure and amyloid burden using [ $^{11}C$ ]PiB PET in aging (non-DS) was investigated by Racine et al. (2014) and found paradoxical increased FA and decreased MD in the PiB(+) group. Subsequently, Wolf et al. (2015) found increased FA and decreased MD accompanying low amyloid plaque burden, but this relationship was reversed for individuals with high amyloid burden, showing decreased FA and increased MD. Increased CSF measured  $A\beta_{42}$  was associated with increased MD in gray and white matter in the frontal, parietal, occipital, and temporal lobes in healthy aging adults at risk for AD (Bendlin et al., 2012). Many, but not all of these areas, show similar patterns of white matter microstructural changes emerging in our DS cohort.

The observed pattern of diffuse DTI changes within the association white matter in the neocortex is consistent with the earliest expected amyloid- $\beta$  accumulation spatial patterns described by (Thal et al., 2002). Ultimately, it would be interesting to better understand how these white matter changes are associated with specific areas of amyloid accumulation. The interaction of age with amyloid load here does create challenges for being specific to amyloid load. Future studies using tractography (beyond the scope of this study) in a larger sample of age-matched amyloid(-) and amyloid(+) cohorts will be needed to relate

the spatial distribution of white matter microstructural changes to amyloid accumulation in cortical gray matter regions.

A potential contributing factor explaining our findings is the presence of cerebrovascular disease, particularly microbleeds (MB). MBs have been observed to occur at a higher rate in individuals with DS and contribute to increased cerebral amyloid angiopathy (CAA) (Head et al., 2017; Helman et al., 2019; Lao et al., 2020). MBs and CAA are linked with  $A\beta$  accumulation and AD onset (Noguchi-Shinohara et al., 2017). In non-DS populations, both CAA (Chen et al., 2007) and MBs (Akoudad et al., 2013) have been reported to influence diffusion metrics and indicate signs of decreased WM structural integrity. Since DTI is sensitive to both MBs and AD-related brain changes, our results may reflect the contributions of both cerebrovascular disease and the presence of  $A\beta$  plaques.

We originally investigated a stratified amyloid(-) versus amyloid(+) analysis, but due to significant differences in age distributions (mean age difference =  $12.6 \pm 8.0$  years) and the small amyloid(+) sample size ( $n = 19$ ), meaningful subgroup analyses were not possible in this cohort. This led us to investigate white matter changes in relationship to age and amyloid load. It would be of great scientific interest to disentangle the interactions between amyloid accumulation and changes in white matter microstructure specific to the DS population to potentially infer causality between these neuropathological features. Future work will focus on examining the time course of these processes as additional longitudinal data are acquired.

Our findings of significant diffuse  $A\beta_L$ \*age interactions highlight the complexity of uncoupling DTI, amyloid and age and warrant further study within DS and non-DS subjects alike. Since both DTI and amyloid measures are related to aging, larger, longitudinal cohort studies with more balanced age distributions will be required to disambiguate age and amyloid burden effects on DTI measures. These interaction effects, however, suggest that increased amyloid burden is associated with more rapid age-related changes in white matter microstructure.

#### Funding

The authors would like to thank the participants and their families for their time and commitment to further discovery and understanding of the causes of AD in Down syndrome. Funding was provided by the following National Institutes of Health grants: R01AG031110, U01AG0514.

This study was also supported in part by a core grant to the Waisman Center from the Eunice Kennedy Shriver national Institute of Child Health and Human Development (U54 HD090256).

Austin Bazydlo was supported by NIH Award Number T32CA009206. The content is solely the responsibility of the authors and does not necessarily represent the official views of the National Institutes of Health.

#### CRediT authorship contribution statement

**Austin M. Bazydlo:** Conceptualization, Methodology, Visualization, Investigation, Formal analysis, Writing – original draft, Writing – review & editing. **Matthew D. Zammit:** Investigation, Formal analysis, Methodology, Writing – review & editing. **Minjie Wu:** Writing – review & editing. **Patrick J. Lao:** Douglas C. Dean: Writing – review & editing, Methodology. **Sterling C. Johnson:** Writing – review & editing. **Dana L. Tudorascu:** Writing – review & editing, Methodology. **Ann Cohen:** Writing – review & editing. **Karly A. Cody:** Writing – review & editing. **Beau Ances:** Writing – review & editing. **Charles M. Laymon:** Writing – review & editing. **William E. Klunk:** Funding acquisition, Writing – review & editing. **Shahid Zaman:** Writing – review & editing. **Benjamin L. Handen:** Writing – review & editing. **Sigan L. Hartley:** Writing – review & editing. **Andrew L. Alexander:** Writing – original draft, Writing – review & editing, Supervision, Methodology, Conceptualization. **Bradley T. Christian:** Writing – review & editing, Writing –

original draft, Project administration, Supervision, Funding acquisition, Methodology, Conceptualization.

## Declaration of Competing Interest

The authors declare the following financial interests/personal relationships which may be considered as potential competing interests: GE Healthcare holds a license agreement with the University of Pittsburgh based on the PiB PET technology described in this manuscript. Dr. Klunk is a co-inventor of PiB and, as such, has a financial interest in this license agreement. GE Healthcare provided no grant support for this study and had no role in the design or interpretation of results or preparation of this manuscript. All other authors have no PiB-related conflicts of interest with this work and had full access to all of the data in the study and take responsibility for the integrity of the data and the accuracy of the data analysis.

## References

2012. 2012. Down Syndrome: Condition Information. NIH.
- Abe, O., Aoki, S., Hayashi, N., Yamada, H., Kunimatsu, A., Mori, H., Yoshikawa, T., Okubo, T., Ohtomo, K., 2002. Normal aging in the central nervous system: quantitative MR diffusion-tensor analysis. *Neurobiol. Aging* 23, 433–441.
- Akoudad, S., de Groot, M., Koudstaal, P.J., van der Lugt, A., Niessen, W.J., Hofman, A., Ikram, M.A., Vernooij, M.W., 2013. Cerebral microbleeds are related to loss of white matter structural integrity. *Neurology* 81, 1930–1937.
- Alexander, A.L., Lee, J.E., Lazar, M., Field, A.S., 2007. Diffusion tensor imaging of the brain. *Neurotherapeutics* 4, 316–329.
- Andersson, J.L.R., Graham, M.S., Zsoldos, E., Sotiropoulos, S.N., 2016. Incorporating outlier detection and replacement into a non-parametric framework for movement and distortion correction of diffusion MR images. *Neuroimage* 141, 556–572.
- Andersson, J.L.R., Sotiropoulos, S.N., 2016. An integrated approach to correction for off-resonance effects and subject movement in diffusion MR imaging. *Neuroimage* 125, 1063–1078.
- Annus, T., Wilson, L.R., Hong, Y.T., Acosta-Cabrero, J., Fryer, T.D., Cardenas-Blanco, A., Smith, R., Boros, I., Coles, J.P., Aigbirhio, F.I., Menon, D.K., Zaman, S.H., Nestor, P.J., Holland, A.J., 2016. The pattern of amyloid accumulation in the brains of adults with Down syndrome. *Alzheimers Dement* 12, 538–545.
- Basser, P.J., Mattiello, J., LeBihan, D., 1994. MR diffusion tensor spectroscopy and imaging. *Biophys. J.* 66, 259–267.
- Basser, P.J., Pierpaoli, C., 1996. Microstructural and physiological features of tissues elucidated by quantitative-diffusion-tensor MRI. *J Magn Reson B* 111, 209–219.
- Beery, K.E., 2004. Beery VMI: The Beery-Buktenica Developmental test of Visual-motor Integration. Pearson, Minneapolis, MN.
- Bendlin, B.B., Carlsson, C.M., Johnson, S.C., Zetterberg, H., Blennow, K., Willette, A.A., Okonkwo, O.C., Sodhi, A., Ries, M.L., Birdsill, A.C., Alexander, A.L., Rowley, H.A., Pugliese, L., Asthana, S., Sager, M.A., 2012. CSF T-Tau/Abeta42 predicts white matter microstructure in healthy adults at risk for Alzheimer's disease. *PLoS ONE* 7, e37720.
- Bennett, I.J., Madden, D.J., Vaidya, C.J., Howard, D.V., Howard Jr., J.H., 2010. Age-related differences in multiple measures of white matter integrity: a diffusion tensor imaging study of healthy aging. *Hum. Brain Mapp.* 31, 378–390.
- Caballero, M.A.A., Song, Z., Rubinski, A., Duering, M., Dichgans, M., Park, D.C., Ewers, M., 2020. Age-dependent amyloid deposition is associated with white matter alterations in cognitively normal adults during the adult life span. *Alzheimer's Dementia* 16, 651–661.
- Chang, L.C., Jones, D.K., Pierpaoli, C., 2005. RESTORE: robust estimation of tensors by outlier rejection. *Magn. Reson. Med.* 53, 1088–1095.
- Chao, L.L., DeCarli, C., Kriger, S., Truran, D., Zhang, Y., Laxamana, J., Villeneuve, S., Jagust, W.J., Sanossian, N., Mack, W.J., Chui, H.C., Weiner, M.W., 2013. Associations between white matter hyperintensities and  $\beta$  amyloid on integrity of projection, association, and limbic fiber tracts measured with diffusion tensor MRI. *PLoS ONE* 8, e65175.
- Chen, S.Q., Kang, Z., Hu, X.Q., Hu, B., Zou, Y., 2007. Diffusion tensor imaging of the brain in patients with Alzheimer's disease and cerebrovascular lesions. *J Zhejiang Univ Sci B* 8, 242–247.
- Evenhuis, H.M., 2018. The dementia questionnaire for people with learning disabilities. In: Prasher, V.P. (Ed.), *Neuropsychological Assessments of Dementia in Down Syndrome and Intellectual Disabilities*. Springer International Publishing, Cham, pp. 43–56.
- Fenoll, R., Pujol, J., Esteba-Castillo, S., de Sola, S., Ribas-Vidal, N., Garcia-Alba, J., Sanchez-Benavides, G., Martinez-Vilavella, G., Deus, J., Dierssen, M., Novell-Alsina, R., de la Torre, R., 2017. Anomalous white matter structure and the effect of age in Down syndrome patients. *J Alzheimers Dis.* 57, 61–70.
- Garyfallidis, E., Brett, M., Amirbekian, B., Rokem, A., van der Walt, S., Descoteaux, M., Nimmo-Smith, I., Dipy, C., 2014. Dipy, a library for the analysis of diffusion MRI data. *Front. Neuroinform.* 8, 8.
- Hartley, S.L., Handen, B.L., Devenny, D.A., Hardison, R., Mihaila, I., Price, J.C., Cohen, A.D., Klunk, W.E., Mailick, M.R., Johnson, S.C., Christian, B.T., 2014. Cognitive functioning in relation to brain amyloid-beta in healthy adults with Down syndrome. *Brain* 137, 2556–2563.
- Haxby, J.V., 1989a. Neuropsychological evaluation of adults with Down's syndrome: patterns of selective impairment in non-demented old adults. *J. Ment. Defic. Res.* 33 (Pt 3), 193–210.
- Haxby, J.V., 1989b. Neuropsychological evaluation of adults with Down's syndrome: patterns of selective impairment in non-demented old adults. *J. Intellect. Disabil. Res.* 33, 193–210.
- Head, E., Phelan, M.J., Doran, E., Kim, R.C., Poon, W.W., Schmitt, F.A., Lott, I.T., 2017. Cerebrovascular pathology in Down syndrome and Alzheimer disease. *Acta Neuropathol. Commun.* 5, 93.
- Helman, A.M., Siever, M., McCarty, K.L., Lott, I.T., Doran, E., Abner, E.L., Schmitt, F.A., Head, E., 2019. Microbleeds and cerebral amyloid angiopathy in the brains of people with down syndrome with Alzheimer's disease. *J. Alzheimers Dis.* 67, 103–112.
- Hsu, J.L., Leemans, A., Bai, C.H., Lee, C.H., Tsai, Y.F., Chiu, H.C., Chen, W.H., 2008. Gender differences and age-related white matter changes of the human brain: a diffusion tensor imaging study. *Neuroimage* 39, 566–577.
- Jack Jr., C.R., Bennett, D.A., Blennow, K., Carrillo, M.C., Dunn, B., Haeberlein, S.B., Holtzman, D.M., Jagust, W., Jessen, F., Karlawish, J., Liu, E., Molinuevo, J.L., Montine, T., Phelps, C., Rankin, K.P., Rowe, C.C., Scheltens, P., Siemers, E., Snyder, H.M., Sperling, R., Contributors, 2018. NIA-AA Research Framework: Toward a biological definition of Alzheimer's disease. *Alzheimers Dement.* 14, 535–562.
- Jenkinson, M., Beckmann, C.F., Behrens, T.E., Woolrich, M.W., Smith, S.M., 2012. Fsl. *Neuroimage* 62, 782–790.
- Jozsvai, E., Hewitt, S., Gedye, A., 2018. Gedye dementia scale for Down Syndrome. In: Prasher, V.P. (Ed.), *Neuropsychological Assessments of Dementia in Down Syndrome and Intellectual Disabilities*. Springer International Publishing, Cham, pp. 57–71.
- Kellner, E., Dhital, B., Kiselev, V.G., Reiser, M., 2016. Gibbs-ring artifact removal based on local subvoxel-shifts. *Magn. Reson. Med.* 76, 1574–1581.
- Klunk, W.E., Engler, H., Nordberg, A., Wang, Y., Blomqvist, G., Holt, D.P., Bergstrom, M., Savitcheva, I., Huang, G.F., Estrada, S., Ausen, B., Debnath, M.L., Barletta, J., Price, J.C., Sandell, J., Lopresti, B.J., Wall, A., Koivisto, P., Antoni, G., Mathis, C.A., Langstrom, B., 2004. Imaging brain amyloid in Alzheimer's disease with Pittsburgh Compound-B. *Ann. Neurol.* 55, 306–319.
- Korkman, M., Kirk, U., Kemp, S., 2007. NEPSY II: Clinical and Interpretive Manual. Harcourt Assessment. PsychCorp.
- Lao, P.J., Betthauser, T.J., Hillmer, A.T., Price, J.C., Klunk, W.E., Mihaila, I., Higgins, A.T., Bulova, P.D., Hartley, S.L., Hardison, R., Tumuluru, R.V., Murali, D., Mathis, C.A., Cohen, A.D., Barnhart, T.E., Devenny, D.A., Mailick, M.R., Johnson, S.C., Handen, B.L., Christian, B.T., 2016. The effects of normal aging on amyloid-beta deposition in nondemented adults with Down syndrome as imaged by carbon 11-labeled Pittsburgh compound B. *Alzheimers Dement.* 12, 380–390.
- Lao, P.J., Gutierrez, J., Keator, D., Rizvi, B., Banerjee, A., Igwe, K.C., Laing, K.K., Sathishkumar, M., Moni, F., Andrews, H., Krinsky-McHale, S., Head, E., Lee, J.H., Lai, F., Yassa, M.A., Rosas, H.D., Silverman, W., Lott, I.T., Schupf, N., Brickman, A.M., 2020. Alzheimer-related cerebrovascular disease in Down syndrome. *Ann. Neurol.* 88, 1165–1177.
- Lao, P.J., Handen, B.L., Betthauser, T.J., Mihaila, I., Hartley, S.L., Cohen, A.D., Tudorascu, D.L., Bulova, P.D., Lopresti, B.J., Tumuluru, R.V., Murali, D., Mathis, C.A., Barnhart, T.E., Stone, C.K., Price, J.C., Devenny, D.A., Johnson, S.C., Klunk, W.E., Christian, B.T., 2018. Alzheimer-like pattern of hypometabolism emerges with elevated amyloid-beta burden in Down syndrome. *J. Alzheimers Dis.* 61, 631–644.
- Lopresti, B.J., Klunk, W.E., Mathis, C.A., Hoge, J.A., Ziolkowski, S.K., Lu, X., Meltzer, C.C., Schimmel, K., Tsopoulos, N.D., DeKosky, S.T., Price, J.C., 2005. Simplified quantification of Pittsburgh Compound B amyloid imaging PET studies: a comparative analysis. *J. Nucl. Med.* 46, 1959–1972.
- Matthews, D.C., Lukic, A.S., Andrews, R.D., Marendic, B., Brewer, J., Rissman, R.A., Mosconi, L., Strother, S.C., Wernick, M.N., Mobley, W.C., Ness, S., Schmidt, M.E., Rafii, M.S., 2016. Dissociation of Down syndrome and Alzheimer's disease effects with imaging. *Alzheimer's Dementia: Transl. Res. Clin. Interventions* 2, 69–81.
- Mayo, C.D., Garcia-Barrera, M.A., Mazerolle, E.L., Ritchie, L.J., Fisk, J.D., Gawryluk, J.R., Alzheimer's Disease Neuroimaging, I., 2018. Relationship between DTI metrics and cognitive function in Alzheimer's disease. *Front. Aging Neurosci.* 10, 436.
- Mayo, C.D., Mazerolle, E.L., Ritchie, L., Fisk, J.D., Gawryluk, J.R., Alzheimer's Disease Neuroimaging, I., 2017. Longitudinal changes in microstructural white matter metrics in Alzheimer's disease. *Neuroimage Clin.* 13, 330–338.
- McCarron, M., McCallion, P., Reilly, E., Mulryan, N., 2014. A prospective 14-year longitudinal follow-up of dementia in persons with Down syndrome. *J. Intellect. Disabil. Res.* 58, 61–70.
- McNamee, R.L., Yee, S.-H., Price, J.C., Klunk, W.E., Rosario, B., Weissfeld, L., Ziolkowski, B., Berginc, M., Lopresti, B., DeKosky, S., Mathis, C.A., 2009. Consideration of optimal time window for Pittsburgh compound B PET summed uptake measurements. *J. Nucl. Med.* 50, 348–355.
- Neale, N., Padilla, C., Fonseca, L.M., Holland, T., Zaman, S., 2018. Neuroimaging and other modalities to assess Alzheimer's disease in Down syndrome. *Neuroimage Clin.* 17, 263–271.
- Noguchi-Shinohara, M., Komatsu, J., Samuraki, M., Matsunari, I., Ikeda, T., Sakai, K., Hamaguchi, T., Ono, K., Nakamura, H., Yamada, M., 2017. Cerebral amyloid angiopathy-related microbleeds and cerebrospinal fluid biomarkers in Alzheimer's disease. *J. Alzheimers Dis.* 55, 905–913.
- Nowrangi, M.A., Lyketsos, C.G., Leoutsakos, J.M., Oishi, K., Albert, M., Mori, S., Mielke, M.M., 2013. Longitudinal, region-specific course of diffusion tensor imaging measures in mild cognitive impairment and Alzheimer's disease. *Alzheimers Dement.* 9, 519–528.

- Nowrangi, M.A., Okonkwo, O., Lyketsos, C., Oishi, K., Mori, S., Albert, M., Mielke, M.M., 2015. Atlas-based diffusion tensor imaging correlates of executive function. *J. Alzheimers Dis.* 44, 585–598.
- O'Dwyer, L., Lamberton, F., Bokde, A.L., Ewers, M., Faluyi, Y.O., Tanner, C., Mazoyer, B., O'Neill, D., Bartley, M., Collins, D.R., Coughlan, T., Prvulovic, D., Hampel, H., 2011. Multiple indices of diffusion identifies white matter damage in mild cognitive impairment and Alzheimer's disease. *PLoS ONE* 6, e21745.
- Powell, D., Caban-Holt, A., Jicha, G., Robertson, W., Davis, R., Gold, B.T., Schmitt, F.A., Head, E., 2014. Frontal white matter integrity in adults with Down syndrome with and without dementia. *Neurobiol. Aging* 35, 1562–1569.
- Price, J.C., Klunk, W.E., Lopresti, B.J., Lu, X., Hoge, J.A., Ziolkowski, S.K., Holt, D.P., Meltzer, C.C., DeKosky, S.T., Mathis, C.A., 2005. Kinetic modeling of amyloid binding in humans using PET imaging and Pittsburgh Compound-B. *J. Cereb. Blood Flow Metab.* 25, 1528–1547.
- Racine, A.M., Adluru, N., Alexander, A.L., Christian, B.T., Okonkwo, O.C., Oh, J., Cleary, C.A., Birdsill, A., Hillmer, A.T., Murali, D., Barnhart, T.E., Gallagher, C.L., Carlsson, C.M., Rowley, H.A., Dowling, N.M., Asthana, S., Sager, M.A., Bendlin, B.B., Johnson, S.C., 2014. Associations between white matter microstructure and amyloid burden in preclinical Alzheimer's disease: a multimodal imaging investigation. *Neuroimage Clin.* 4, 604–614.
- Raffi, M.S., Wishnek, H., Brewer, J.B., Donohue, M.C., Ness, S., Mobley, W.C., Aisen, P.S., Rissman, R.A., 2015. The down syndrome biomarker initiative (DSBI) pilot: proof of concept for deep phenotyping of Alzheimer's disease biomarkers in down syndrome. *Front. Behav. Neurosci.* 9, 239.
- Romano, A., Moraschi, M., Cornia, R., Bozzao, A., Rossi-Espagnet, M.C., Giove, F., Albertini, G., Pierallini, A., 2018. White matter involvement in young non-demented Down's syndrome subjects: a tract-based spatial statistic analysis. *Neuroradiology* 60, 1335–1341.
- Smith, S.M., Jenkinson, M., Johansen-Berg, H., Rueckert, D., Nichols, T.E., Mackay, C.E., Watkins, K.E., Ciccarelli, O., Cader, M.Z., Matthews, P.M., Behrens, T.E., 2006. Tract-based spatial statistics: voxelwise analysis of multi-subject diffusion data. *Neuroimage* 31, 1487–1505.
- Smith, S.M., Jenkinson, M., Woolrich, M.W., Beckmann, C.F., Behrens, T.E., Johansen-Berg, H., Bannister, P.R., De Luca, M., Drobnjak, I., Flitney, D.E., Niazy, R.K., Saunders, J., Vickers, J., Zhang, Y., De Stefano, N., Brady, J.M., Matthews, P.M., 2004. Advances in functional and structural MR image analysis and implementation as FSL. *Neuroimage* 23 (Suppl 1), S208–219.
- Smith, S.M., Nichols, T.E., 2009. Threshold-free cluster enhancement: addressing problems of smoothing, threshold dependence and localisation in cluster inference. *Neuroimage* 44, 83–98.
- Sparrow, S.S., Balla, D.A., Cicchetti, D.V., Harrison, P.L., 1984. Vineland adaptive behavior scales.
- Thal, D.R., Rub, U., Orantes, M., Braak, H., 2002. Phases of A beta-deposition in the human brain and its relevance for the development of AD. *Neurology* 58, 1791–1800.
- Tournier, J.D., Smith, R., Raffelt, D., Tabbara, R., Dhollander, T., Pietsch, M., Christiaens, D., Jeurissen, B., Yeh, C.H., Connelly, A., 2019. MRtrix3: A fast, flexible and open software framework for medical image processing and visualisation. *Neuroimage* 202, 116137.
- Veraart, J., Novikov, D.S., Christiaens, D., Ades-Aron, B., Sijbers, J., Fieremans, E., 2016. Denoising of diffusion MRI using random matrix theory. *Neuroimage* 142, 394–406.
- Wechsler, D., 1945. **Wechsler memory scale.**
- Wiseman, F.K., Al-Janabi, T., Hardy, J., Karmiloff-Smith, A., Nizetic, D., Tybulewicz, V.L.J., Fisher, E.M.C., Strydom, A., 2015. A genetic cause of Alzheimer disease: mechanistic insights from Down syndrome. *Nat. Rev. Neurosci.* 16, 564–574.
- Wolf, D., Fischer, F.U., Scheurich, A., Fellgiebel, A., Alzheimer's Disease Neuroimaging, I., 2015. Non-linear association between cerebral amyloid deposition and white matter microstructure in cognitively healthy older adults. *J. Alzheimers Dis.* 47, 117–127.
- Woods, R.P., Grafton, S.T., Holmes, C.J., Cherry, S.R., Mazziotta, J.C., 1998. Automated image registration: I. General methods and intrasubject, intramodality validation. *J. Comput. Assist. Tomogr.* 22, 139–152.
- Zammit, M.D., Laymon, C.M., Betthausen, T.J., Cody, K.A., Tudorascu, D.L., Minhas, D.S., Sabbagh, M.N., Johnson, S.C., Zaman, S.H., Mathis, C.A., Klunk, W.E., Handen, B.L., Cohen, A.D., Christian, B.T., 2020a. Amyloid accumulation in Down syndrome measured with amyloid load. *Alzheimers Dement. (Amst)* 12, e12020.
- Zammit, M.D., Laymon, C.M., Tudorascu, D.L., Hartley, S.L., Piro-Gambetti, B., Johnson, S.C., Stone, C.K., Mathis, C.A., Zaman, S.H., Klunk, W.E., Handen, B.L., Cohen, A.D., Christian, B.T., 2020b. Patterns of glucose hypometabolism in Down syndrome resemble sporadic Alzheimer's disease except for the putamen. *Alzheimer's Dementia: Diagnosis Assessment Dis. Monitor.* 12, e12138.
- Zigman, W.B., Devenny, D.A., Krinsky-McHale, S.J., Jenkins, E.C., Urv, T.K., Wegiel, J., Schupf, N., Silverman, W., 2008. Chapter 4 Alzheimer's Disease in Adults with Down Syndrome. *International Review of Research in Mental Retardation.* Academic Press, pp. 103–145.